

Exact dynamical solution of the Kuramoto–Sakaguchi Model for finite networks of identical oscillators

Antonio Mihara and Rene O. Medrano-T *

Departamento de Física, UNIFESP - Universidade Federal de São Paulo
Rua São Nicolau, 210, 09913-030, Diadema SP, Brazil

May 4, 2018

Abstract

We study the Kuramoto–Sakaguchi (KS) model composed by any N identical phase oscillators symmetrically coupled. Ranging from local (one-to-one, $R = 1$) to global (all-to-all, $R = N/2$) couplings, we derive the general solution that describes the network dynamics next to an equilibrium. Therewith we build stability diagrams according to N and R bringing to the light a rich scenery of attractors, repellers, saddles, and non-hyperbolic equilibriums. Our result also uncovers the obscure repulsive regime of the KS model through bifurcation analysis. Moreover, we present numerical evolutions of the network showing the great accordance with our analytical one. The exact knowledge of the behavior close to equilibriums is a fundamental step to investigate phenomena about synchronization in networks. As an example, at the end we discuss the dynamics behind chimera states from the point of view of our results.

Introduction

For more than forty years, the paradigmatic system of N one-dimensional coupled phase oscillators, the Kuramoto model [1], has been intensively studied to understand phenomena related to synchronization in biological, chemical, and electronic networks. Despite the simplicity of the dynamics of each oscillator ($\dot{\theta} = \omega$) strong efforts should be dedicated to find analytical solutions for a network of nonlinearly coupled oscillators, due to the high dimensionality of the system. Kuramoto showed a seminal solution giving rise to the prosper application of the mean–field theory in the Kuramoto model [2]. The method considers the network in the thermodynamic limit $N \rightarrow \infty$ with oscillators globally coupled. So that, the network is described oscillating with a mean frequency and its coherence is given by the magnitude of an order parameter. Since then this approach has been largely well succeeded in analytical investigations [2, 3, 4, 5, 6, 7, 8, 9]. In contrast, accurate results for the finite-size Kuramoto model remains a challenge due to the great number of equations involved, nevertheless, the dynamics is richer. While in the global coupling the full synchronization is the only stable equilibrium, in different topologies of the Kuramoto model multistability is allowed [10]. And, sustained by Lyapunov function argument, the system would reach an equilibrium state as $t \rightarrow \infty$ [11]. In this context, equilibriums play a central role in the network dynamics.

Multistability [12, 13], basin of attractions [14, 15], and traveling waves [16] are some of fundamental phenomena directly related with equilibriums in variants of the Kuramoto model with both attractive and repulsive phase couplings¹. These phenomena are also observed in real-world networks [17, 18, 19, 20]. Such manifestations are mostly studied in the continuous thermodynamic limit and keep not yet well understood. Exact solutions for lower number of oscillators in the Kuramoto model are mandatory in this study but they are still a topic of investigation [21, 22]. In order to shed some light on those problems we study a class of the Kuramoto–Sakaguchi (KS) model [23], a generalization of the Kuramoto model explicitly for finite N . We obtain solutions that describe precisely the trajectories of each oscillators of the network when the system is close

*E-mails: mihara74@gmail.com, rene.medrano@unifesp.br.

¹The dynamics of networks with repulsive phase couplings is almost unknown in spite its relevance in neurons networks. In the repulsive regime, the oscillators do not collapse in a single phase although they synchronize in frequency.

to an equilibrium. The collective time evolution of the network can be followed by the order parameter [8] but this is the first time that the evolution of the network elements can be individually described analytically. We present several studies comparing numerical simulations with our theoretical predictions.

KS model is given by

$$\dot{\theta}_{\mathbf{x}} = \omega_{\mathbf{x}} + \sum_{\langle \mathbf{y}, \mathbf{x} \rangle} G(\mathbf{x}, \mathbf{y}) \sin(\theta_{\mathbf{y}} - \theta_{\mathbf{x}} - \alpha), \quad (1)$$

where $\mathbf{x} = 0, 1, 2, \dots, N - 1$ identifies the \mathbf{x} -th oscillator in a ring, $\omega_{\mathbf{x}}$, its natural frequency, and $G(\mathbf{x}, \mathbf{y})$, the coupling rule between it and the \mathbf{y} -th oscillator. The notation $\langle \mathbf{y}, \mathbf{x} \rangle$ means that the summation is on the R nearest neighbors in both sides of oscillator \mathbf{x} , then \mathbf{y} assumes the values $\mathbf{x} - R, \mathbf{x} - R + 1, \dots, \mathbf{x}, \dots, \mathbf{x} + R$, where R can be from $R = 1$ (*local coupling*) to $R = (N - 1)/2$ (*global coupling*), if N is odd. If $1 < R < (N - 1)/2$ the coupling is called *nonlocal*. Finally, $\alpha \in (-\pi, \pi]$ is a constant that, for positive coupling, determines the regime of the network named *attractive* if $|\alpha| < \pi/2$ and *repulsive* otherwise.

Considering N identical oscillators ($\omega_{\mathbf{x}} = \text{constant}, \forall \mathbf{x}$) interacting according to KS model, with periodic boundary conditions, as in general studies of chimera states [24, 25, 26] (for the case $\omega_{\mathbf{x}} \neq \omega_{\mathbf{y}}$ see [22]), an equilibrium is related to the phase difference between the nearest neighbors of oscillators $\Delta = \theta_{\mathbf{x}+1} - \theta_{\mathbf{x}}$. Due to the similarity, any homogeneous phase distribution of the oscillators along of a circle is an equilibrium, i.e.,

$$\Delta = \frac{2\pi}{N}q, \quad q = 0, 1, 2, \dots, N - 1. \quad (2)$$

The integer number q denotes the number of loops needed to distribute the phase oscillators in the circle. The trivial solution is $\Delta = 0$ (or 2π) corresponding to the full synchronization. For the rest ($q \neq 0$) we say that the network is synchronized in a *q-twisted state*. Note there are no different distribution for $q \geq N$. In this work we describe rigorously the stability properties of the *q-twisted states* assuming a general symmetric coupling $G(|\mathbf{y} - \mathbf{x}|) \equiv G_n$, only dependent on the absolute distance between oscillators, $n = \mathbf{y} - \mathbf{x}$. More specifically, we determine the set of eigenvalues associated to each state identifying the complete stability scenario of hyperbolic and non-hyperbolic equilibriums for a finite number N of oscillators. As an application we show specifically this scenery in the parameter space $R \times q$ of the repulsive regime and calculate the bifurcation of twisted states in the thermodynamic limit. In the end we discuss how these results contribute to a dynamical interpretation of chimera states.

Results

Synchronization frequency of *q*-twisted states

Without loss of generality we assume that frequency $\omega_{\mathbf{x}} = 0$, periodic boundary conditions ($\theta_0 = \theta_N$) and N odd. Then Eq. (1) can be rewritten as

$$\dot{\theta}_{\mathbf{x}} = \sum_{n=-R}^R G_n \sin(\theta_{\mathbf{x}+n} - \theta_{\mathbf{x}} - \alpha). \quad (3)$$

Based on the system symmetry, we assume that the network shall asymptotically converge to a *q-twisted state* with the same constant frequency $\dot{\theta}_{\mathbf{x}} = \Omega$. Assuming $\theta_0 = 0$, we obtain $\theta_{\mathbf{x}} = \Omega t + \Delta \mathbf{x}$. Substituting this result in Eq. (3), the network synchronization frequency Ω of any mode q is obtained:

$$\Omega = \sum_{n=-R}^R G_n \sin(n\Delta - \alpha). \quad (4)$$

Analysis of Stability

We begin to analyze the stability of *q-twisted states* by taking into account a small perturbation in its solution : $\theta_{\mathbf{x}} = \Omega t + \Delta \mathbf{x} + \mathcal{E}_{\mathbf{x}}$. Then

$$\dot{\theta}_{\mathbf{x}} = \Omega + \dot{\mathcal{E}}_{\mathbf{x}} \quad (5)$$

Substituting Eq.(5) in the LHS of Eq.(3) and expanding the (perturbed) RHS of Eq.(3) to first order in \mathcal{E}_x we obtain (with $\psi \equiv n\Delta - \alpha$)

$$\dot{\mathcal{E}}_x(t) = \sum_{n=-R}^R G_n \cos \psi (\mathcal{E}_{x+n} - \mathcal{E}_x). \quad (6)$$

With the ansatz $\mathcal{E}_x(t) = \mathcal{A}_x e^{\lambda t}$, (or with vector notation: $\vec{\mathcal{E}}(t) = \vec{A} e^{\lambda t}$), Eq.(6) becomes

$$\begin{aligned} \lambda \mathcal{A}_x &= \sum_{n=-R}^R G_n \cos(\psi) (\mathcal{A}_{x+n} - \mathcal{A}_x) \\ &= \sum_{n=1}^R G_n [\rho_n \mathcal{A}_{x-n} + \mu_n \mathcal{A}_{x+n}] - \beta \mathcal{A}_x \end{aligned} \quad (7)$$

where $\rho_n = \cos(n\Delta + \alpha)$, $\mu_n = \cos(n\Delta - \alpha)$, and

$$\beta = \sum_{n=1}^R G_n (\rho_n + \mu_n) = 2 \cos \alpha \sum_{n=1}^R G_n \cos(n\Delta) \quad (8)$$

The eigenvalue Eq. (7) can be written in the matrix form $\lambda \vec{A} = M \vec{A}$, where $\vec{A} = [\mathcal{A}_0, \dots, \mathcal{A}_x, \dots, \mathcal{A}_{N-1}]^T$ and M is a circulant matrix [27]

$$M = \begin{pmatrix} -\beta & G_1 \mu_1 & G_2 \mu_2 & \cdots & G_2 \rho_2 & G_1 \rho_1 \\ G_1 \rho_1 & -\beta & G_1 \mu_1 & \cdots & G_3 \rho_3 & G_2 \rho_2 \\ G_2 \rho_2 & G_1 \rho_1 & -\beta & \cdots & G_4 \rho_4 & G_3 \rho_3 \\ \vdots & \vdots & \vdots & \vdots & \ddots & \vdots \\ G_1 \mu_1 & G_2 \mu_2 & G_3 \mu_3 & \cdots & G_1 \rho_1 & -\beta \end{pmatrix} \quad (9)$$

with (non-normalized) eigenvectors given by

$$\begin{aligned} \vec{A}_\ell &= [z_\ell^0, \dots, z_\ell^x, \dots, z_\ell^{N-1}]^T, \\ z_\ell &\equiv \exp\left(i \frac{2\pi}{N} \ell\right), \end{aligned} \quad (10)$$

with $\ell = 0, 1, 2, \dots, N-1$.

The ℓ -th eigenvalue of the q -twisted state is given by $\lambda_\ell = \gamma_\ell + i\varpi_\ell$, with

$$\gamma_\ell = -4 \cos \alpha \sum_{k=1}^R G_k \cos\left(k \frac{2\pi}{N} q\right) \sin^2\left(k \frac{\pi}{N} \ell\right) \quad (11)$$

$$\varpi_\ell = 2 \sin \alpha \sum_{k=1}^R G_k \sin\left(k \frac{2\pi}{N} q\right) \sin\left(k \frac{2\pi}{N} \ell\right). \quad (12)$$

Any perturbation $\vec{\mathcal{E}}(t)$ can be written in terms of the eigenmodes: $\vec{\mathcal{E}}(t) = \sum_\ell C_\ell \vec{F}_\ell(t)$, with $\vec{F}_\ell(t) = \vec{A}_\ell e^{\lambda_\ell t}$ or, without vector notation, $\mathcal{E}_x(t) = \sum_\ell C_\ell F_\ell(x, t)$ where $F_\ell(x, t) = z_\ell^x e^{\lambda_\ell t}$ which is a wave function:

$$F_\ell(x, t) = e^{\gamma_\ell t} \exp\left\{i \left[\frac{2\pi \ell}{N} x + \varpi_\ell t \right]\right\}. \quad (13)$$

Notice that the eigenmode $\ell = 0$, with eigenvalue $\lambda_0 = 0$ and eigenvector $\vec{A}_0 = [1, 1, \dots, 1]^T$, results from the invariance of the system given Eq.(1) under a global phase shift: $\theta_x \rightarrow \theta_x + C$, $\forall \mathbf{x}$. Then, despite of the N equations following Eq. (1), the equilibriums are $(N-1)$ -dimensional since they are related to the phase difference. In other words, the sum of all phase differences is a multiple of 2π due to the periodic boundary condition such that any phase difference can be obtained from the others $N-1$. Therefore the eigenmode $\ell = 0$ shall be disregarded below.

Testing our results

In order to test our results, we confronted them with some “brute force” numerical simulations. In one of many simulations we evolved a network of 50 oscillators locally coupled ($R = 1$) with $\alpha = 1.5$ and $G_n = 0.1$. The time evolution of such a system was performed by direct numerical integration of the 50 differential equations (Eq.(3)) from random initial conditions and the system reached a twisted state with $q = 8$: the system has frequency synchronization, i.e. all the oscillators have the same phase velocity $\Omega = -0.20665$, and the phase difference between any two neighbors is $\theta_{\mathbf{x}} - \theta_{\mathbf{x}-1} = 8.(2\pi/50)$, $\forall \mathbf{x}$.

Regarding the theoretic aspect, for $q = 8$ we can compute all the (real part of) eigenvalues (only for $\ell > 0$) with Eq.(11):

$$\begin{aligned}\gamma_1 &= \gamma_{49} \approx -0.598 \times 10^{-4}, \\ \gamma_2 &= \gamma_{48} \approx -2.38 \times 10^{-4}, \\ \gamma_3 &= \gamma_{47} \approx -5.32 \times 10^{-4}, \\ &\dots \\ \gamma_{24} &= \gamma_{26} \approx -151. \times 10^{-4}, \\ \gamma_{25} &\approx -152. \times 10^{-4}.\end{aligned}$$

We observe that all $\gamma_{\ell(>0)}$ are negative and, as we shall discuss in the next subsection, it is a clear signal that the 8-twisted state is stable, in agreement with the numerical simulation. On the other hand if we assume that the lifetime of an eigenmode can be estimated as $\tau_{\ell} \sim |\gamma_{\ell}|^{-1}$, clearly the eigenmodes $\ell = 1$ and 49 have the longest lifetimes.

For large times, but before the system reaches the final state $q = 8$, it is reasonable to expect a behavior dominated by the eigenmodes $\ell = 1, 49$ of the 8-twisted state: a wave (Eq. (13)) with amplitude decaying exponentially with constant $\gamma = \gamma_{1,49}$. Substituting the parameters of the network in Eqs.(4, 12) we obtain, respectively, $\Omega_8 = -0.20665$ and $\varpi_1 = |\varpi_{49}| = 0.0211 \equiv \omega_T$.

In Fig.1 we show the behavior of θ_{25} (the phase velocity of the oscillator in the site $\mathbf{x} = 25$) for $80000 \leq t \lesssim 96000$ (black line) and its corresponding spectrum. One can observe in Fig.1 that the pronounced peak in the spectrum is around $\omega \approx \omega_T$ (blue line) and the oscillation amplitude of θ_{25} is decaying exponentially to the final synchronization frequency Ω_8 as predicted above: the red curve is obtained with a function proportional to $\exp(\gamma t)$.

Some applications

Stability of states in finite networks

The eigenmodes² are stable if $\gamma_{\ell} < 0$ and unstable if $\gamma_{\ell} > 0$. Thus, a q -twisted state can be classified as:

- (a) **attractor** (hyperbolic) if $\gamma_1, \dots, \gamma_{N-1} < 0$;
- (b) **repeller** (hyperbolic) if $\gamma_1, \dots, \gamma_{N-1} > 0$;
- (c) **saddle** (hyperbolic) if $\exists \gamma_{\ell} \gamma_{\ell'} < 0$;
- (d) **non-hyperbolic** if $\exists \gamma_{\ell} = 0$.

We call the attention for some remarks about the items above. (i) If a non-hyperbolic state has all the other $\gamma_{\ell} < 0$ the system does not converge completely to the q -twisted state however it synchronizes. We call this state as neutrally stable. In the last subsection before the “Discussion” section we show with simulations the different signatures of hyperbolic and non-hyperbolic stable twisted states: the former has a homogeneous phase distribution ($\theta_{\mathbf{x}} - \theta_{\mathbf{x}-1} = \text{constant}$, $\forall \mathbf{x}$) and the latter does not have. (ii) Due to the assumption of periodic boundary conditions there is a symmetry between the stability of $-q$ and q states: The real part of their eigenvalues [Eq. (11)] are the same ($\gamma_q = \gamma_{-q}$). One also can see from Eq.(2) that $-q$ and $N - q$ represent the same state, so there is another way of labeling the twisted states, for instance: $q = -(N-1)/2, \dots, -1, 0, 1, \dots, (N-1)/2$, if N is odd. (iii) If $\alpha = \pi/2$ the eigenvalues are purely imaginary and the stability is not

²Remember that only the eigenmodes with $\ell > 0$ are considered here.

well defined by our assumptions. (iv) Since typically $\varpi_\ell \neq 0$, there are several different types of equilibria with stable and unstable manifolds which we generically call saddle. (v) Although our deduction assumed N odd, the analysis can be easily extended to N even.

As an example, we consider a network of $N = 20$ oscillators in a ring with the same and positive coupling in the repulsive regime ($\pi/2 < |\alpha| \leq \pi$). We varied R from local to global and tested the stability of each q -twisted state according to the sign of $\gamma_\ell, \forall \ell > 0$. The outcome is compiled in Fig. 2.

The stable states are highlighted in (light) blue in our diagrams and they could be compared with those in Fig. 1 of Ref.[13], which were obtained exclusively by direct numerical integration of the Kuramoto equations. The attractors are represented by blue rectangles in the diagrams and the non-hyperbolic (or neutrally) stable states are in light blue.

Due to Eq.(11) and conditions (a-d) above, if we change the system from “attractive” to “repulsive” regime (or vice versa) repellers become attractors and vice versa, including non-hyperbolic equilibria, and saddles keep their unstable character in both regimes. The states with ‘0’ have $\gamma_\ell = 0, \forall \ell$ and our analysis above is unable to determine their stability. However, according to our simulations, such states seem to be unstable in both regimes.

Bifurcations in the continuous limit

Now we analyze the case of a network of oscillators in the continuum limit. We also assume below that each oscillator is coupled to its R nearest neighbors (each side) with constant coupling.

We start with a network locally coupled ($R = 1$). From Eq. (11) the stability of a q -twisted state can change from attractor to repeller (vice versa) according to the sign of $\cos(2\pi q/N)$. For $|q| = N/4$ all eigenvalues are purely imaginary, consequently these states are not asymptotically stable or unstable. Therefore there is a bifurcation point given by the ratio $|q|/N = 1/4$. Since in our representation $|q| \leq (N - 1)/2$, the maximum ratio $|q|/N$ tends to $1/2$ in the limit of $N \rightarrow \infty$. Therefore a network locally coupled presents approximately half of its states as (hyperbolic) attractors and the other half, repellers, independently of α and G_n .

For nonlocal couplings, the stability of the q -twisted states depends only on the ratio R/N . This is clearly expressed in the thermodynamic limit $N \rightarrow \infty$ of Eq. (11) where, in the attractive regime, stable solutions are obtained when

$$\int_0^{R/N} \cos(2\pi qz) \sin^2(\pi lz) dz > 0 \quad (14)$$

in the range $1 \leq R \leq N/2$, for $G_n > 0$ and constant. For a given q -twisted state, its stability changes when the integral in the inequality (14) is null. Defining the function $f(x, y) \equiv \sin(2\pi xy)/y$, with $x = R/N$, to express the solution of the integral, the bifurcation condition is given by

$$f(x, (\ell - q)) - 2f(x, q) + f(x, (\ell + q)) = 0. \quad (15)$$

For a chosen q , we set $\ell = 1$ and vary x from 0 to 0.5 and find values $(x_{q(\ell=1)})$ that solve the equation. This process should be repeated for $\ell = 2, 3, \dots$. Since the stability condition Eq.(14) is satisfied when $x \gtrsim 0$, a q -twisted state loses its stability when Eq. (15) is satisfied for some ℓ , remaining unstable in the rest of the range of x . In our example twist bifurcations happen for $\ell = 1$: $tb_{q(1)} = x_{q(1)}$ (See the middle column in table 1). This result is valid for more complex networks. In [10] the authors obtained the same solution from the mean-field approach considering a symmetric distribution of coupling G_n .

In the repulsive regime, the condition of stability is no longer satisfied when $x \gtrsim 0$ for non-local couplings. So now the first twist bifurcation point demarcates the boundary where a q -twisted state becomes stable. In this regime several twist bifurcation can occur as shown in the last column of table 1. For local couplings, condition becomes $|q|/N > 1/4$.

For any value of R/N , the state of full synchronization ($q = 0$) shall be a hyperbolic attractor in the attractive regime and a hyperbolic repeller in the repulsive regime. On the other hand the numbers in table 1 should be interpreted as follows: **(I)** In the attractive regime, $tb_{q(1)}$ is the highest value of R/N where the q -twisted state is stable. For instance, $tb_{2(1)} = 1/6$ means that the state $q = 2$ is stable for $0 < R/N < 1/6$. **(II)** In the repulsive regime, several values of $tb_{q(\ell)}$ determine ranges of stabilities, for a given q . For instance: $q = 4$ is stable when $tb_{4(9)} < R/N < tb_{4(7)}$ and $tb_{4(2)} < R/N < 0.5$ (green stripes in Fig.3) .

Twisted State	Attractive Regime (I)		Repulsive Regime (II)	
q	ℓ	$tb_{q(\ell)}$	ℓ	$tb_{q(\ell)}$
1	1	0.340461	-	unstable
2	1	1/6	5	0.277562
3	1	0.110727	7	0.191433
			5	0.308065
4	1	0.082948	9	0.145507
			7	0.225577
			2	5/12
5	1	0.066323	11	0.117041
			9	0.178895

Table 1: Bifurcations in the continuum limit.

Time evolution of the Kuramoto order parameter

It is important to remember that our analysis of stability were performed by taking into account a small perturbation \mathcal{E}_x in the q -twisted states. On the other hand with the (real part of the) eigenvalues Eq.(11) one can predict if a given q -twisted state is stable or not, then if the system is “close” to a stable state, the time evolution of each phase can be approximately

$$\theta_x(t) \approx \Omega.t + \Delta.x + \sum_{\ell} C_{\ell} F_{\ell}(x, t), \quad (16)$$

where Ω is the synchronization frequency of the state, given by Eq.(4); $\Delta = 2\pi q/N$ and $F_{\ell}(x, t)$ are the (perturbation) eigenfunctions Eq.13. Eventually the time evolution of the Kuramoto order parameter, for a system close to an attractor, could be predicted directly with our formulas:

$$\rho(t) = \left| \frac{1}{N} \sum_{\mathbf{x}} e^{i\theta_x(t)} \right| \quad (17)$$

We considered a system with the following parameters: $\alpha = 0.4$, $R = 1$, $N = 50$, $K = 1$ and initially in the state $q_0 = 0$, (then $\Delta = 0$, $\forall \mathbf{x}$), with a not too small perturbation:

$$\theta_x(0) = 1.4e^{-(x-25)^2/200} \sin(7.5\pi x/50), \quad (18)$$

with $\mathbf{x} = 0, 1, \dots, 49$.

From the condition above we evaluated the phases by (i) “brute force” numerical integration of the 50 (KS) differential equations (“Simulation”) and by (ii) our theoretical formulation: the initial condition Eq. (18) was decomposed in its Fourier components A_{ℓ}, B_{ℓ} ; Ω and the eigenvalues were obtained with Eqs. (4, 11, 12) for $q = 0$; and the time evolution of each phase was calculated with:

$$\begin{aligned} \theta_x(t) = \Omega t &+ \sum_{\ell} e^{\gamma_{\ell}.t} \left[A_{\ell} \cos \left(\frac{2\pi\ell}{50} .x + \varpi_{\ell}.t \right) \right. \\ &+ \left. B_{\ell} \sin \left(\frac{2\pi\ell}{50} .x + \varpi_{\ell}.t \right) \right]. \end{aligned} \quad (19)$$

Then the Kuramoto order parameter was computed for both cases and the comparison is presented in Fig. 4.

Hyperbolic and Non-hyperbolic Stable States

We show now the differences between hyperbolic and neutrally (or non-hyperbolic) stable states with the results of some simulations.

We simulated the case of a network with $N = 20$ oscillators, $K > 0$, $\alpha = \pi$ (“repulsive” regime), $R = 8$ and a initial configuration “close” to $q = 2$:

$$\theta_x(t = 0) = \mathbf{x} . \frac{2\pi}{20} .2 + r_x, \quad \mathbf{x} = 0, 1, \dots, 19, \quad (20)$$

where r_x is a random number between -0.4 and 0.4.

By numerical integration (2nd order Runge–Kutta, with $\Delta t = 0.025$) we measured the phase velocity ($d\theta_x/dt$) of each oscillator, the phase differences between oscillators and the mean value of q .

The results are presented in Fig.5(a). We can observe in the diagram of Fig.2(b) that ($R = 8, q = 2$) is a **hyperbolic** attractor. We observed that the system reaches a state in which the distribution of phases is homogeneous: $(\theta_x - \theta_{x-1}) = \frac{2\pi}{N}q, \forall x$, in this case $N = 20, q = 2$. We can also observed that $\bar{q} = 2$ during the entire simulation and each oscillator finished with null velocity.

On the other hand in the diagram of Fig.2(b) we can notice that ($R = 9, q = 2$) is a non-hyperbolic neutrally stable state. In order to observe the behavior of such a state we performed another simulation with almost the same conditions of the previous simulation, except with $R = 9$, and the results are presented in Fig.5(b).

As occurred in the previous case, $\bar{q} = 2$ during the entire simulation and each oscillator finished with null velocity. However the system does not reach a state with a homogeneous distribution of phases.

Final remarks

In this work we presented the exact solution of the KS model for finite N number of identical oscillators and give an extended analysis about the stability and the dynamics surround q -twisted states. So that, we are able to characterize precisely the nature around attractors, repellers, saddles and also non-hyperbolic equilibriums, some of the well known most fundamental invariant sets capable to dictate the global behavior in dynamic systems. We expect that this study gives new insights to understand several basic open problems in synchronization. Here we give an example. It is known that in KS models a chimera state (simultaneous manifestation of coherent and incoherent states in a network) collapses to $q = 0$ (full synchronization) state after some time. In order to increase the lifetime without increasing the network, the relation $R/N \approx 0.35$ has been largely employed, seemingly empirically, in studies of chimera states in KS model and in several others different network models based on Rössler, Lorenz, FitzHugh-Nagumo, Stuart-Landau, and Mackey-Glass dynamical systems [28, 29, 30].

According to our results, the bifurcations presented in table 1 indicate that for $R/N \gtrsim 0.34$ only the state $q = 0$ is stable. The other states are unstable, mostly saddles and some repellers. While these equilibriums contribute to the incoherent behavior, the equilibrium $q = 0$ keep some oscillators synchronized. Additionally, if we enhance N and R , but with fixed ratio $R/N \gtrsim 0.34$, there will appear new populations of saddles increasing the ergodicity of the environment and, consequently, extending the chimera lifetime. Such scenery seems to be in agreement with the previous numerical study in the KS model with $R/N \approx 0.35$ and $\alpha = 1.46$ [31]. The authors also observed that the average lifetime of chimeras (before the full synchronization of the network) grows exponentially with N .

Another novelty from our results concerns to the repulsive regime of the KS model. Much attention has been paid to the full synchronization in networks, nevertheless bird flocks, fish schools, activity of cortical neurons in cats, and traveling waves in undulatory locomotion of fishes and lampreys are some of several manifestations in nature strongly related with a kind of synchronization where, contrary to the full synchronization and as in the repulsive regime of the KS model, the units must not approach each other indefinitely. They converge asymptotically to different states resulting in a homogeneous distribution, crucial for the efficient operation of the network. It is impressive that despite of several important advances performed in the paradigmatic KS model its repulsive regime remained almost untouched. With our performed bifurcation study, this work arises the knowledge of the repulsive regime to the same level of the traditional attractive regime concerning the equilibrium states.

Acknowledgements

R.O.M.T thanks M. Zaks and Y. Maistrenko for useful discussions, and acknowledge the support by São Paulo Research Foundation (FAPESP, Proc. 2015/50122-0). The plots were created with Python and its libraries: Matplotlib, Numpy and Scipy.

References

- [1] Y. Kuramoto, *Self-entrainment of a population of coupled non-linear oscillators*. In: H. Arakai (Ed.), International Symposium on Mathematical Problems in Theoretical Physics, Lecture Notes in Physics, vol. 39, Springer, New York, p. 420, 1975.
- [2] Y. Kuramoto, *Chemical Oscillations, Waves, and Turbulence*. Berlin: Springer-Verlag, 1984.
- [3] S. Watanabe and S. H. Strogatz *Phys. Rev. Lett.*, vol. 70, p. 2391, 1993.
- [4] S. H. Strogatz *Physica D*, vol. 143, p. 1, 2000.
- [5] S. H. Strogatz *Nature*, vol. 410, p. 268, 2001.
- [6] J. A. Acebrón, L. L. Bonilla, C. J. P. Vicente, F. Ritort, and R. Spigler *Rev. Mod. Phys.*, vol. 77, p. 137, 2005.
- [7] E. Ott and T. M. Antonsen *Chaos*, vol. 18, p. 037113, 2008.
- [8] O. E. Omel'chenko, M. Wolfrum, and C. R. Laing *Chaos*, vol. 24, p. 023102, 2014.
- [9] X. Hu, S. Boccaletti, W. Huang, X. Zhang, Z. Liu, S. Guan, and C.-H. Lai *Sci. Rep.*, vol. 4, p. 7262, 2014.
- [10] D. A. Wiley and S. H. Strogatz *Chaos*, vol. 16, p. 015103, 2006.
- [11] J. L. Hemmen and W. F. Wreszinski *J. of Stat. Phys.*, vol. 72, p. 145, 1993.
- [12] P. F. C. Tilles, F. F. Ferreira, and H. A. Cerdeira *Phys. Rev. E*, vol. 83, p. 066206, 2011.
- [13] T. Girnyk, M. Hasler, and Y. Maistrenko *Chaos*, vol. 22, p. 013114, 2012.
- [14] R. Delabays, M. Tyloo, and P. Jacquod *Chaos*, vol. 27, p. 103109, 2017.
- [15] S.-Y. Ha and M.-J. Kang *SIAM J. Appl. Math.*, vol. 72, p. 1549, 2012.
- [16] H. Hong and S. H. Strogatz *Phys. Rev. Lett.*, vol. 106, p. 054102, 2011.
- [17] A. H. Cohen, G. B. Ermentrout, T. Kiemel, N. Kopell, K. A. Sigvardte, and T. L. Williams *Trends Neurosci.*, vol. 15, p. 434, 1992.
- [18] G. B. Ermentrout and N. Kopell *SIAM J. Appl. Math.*, vol. 54, p. 478, 1994.
- [19] M. Tsodyks, T. Kenet, A. Grinvald, and A. Arieli *Science*, vol. 286, p. 1943, 1999.
- [20] J. P. Newman and R. J. Butera *Chaos*, vol. 20, p. 023118, 2010.
- [21] J. C. Bronski, L. DeVille, and M. J. Park *Chaos*, vol. 22, p. 033133, 2012.
- [22] C. Wang, N. Rubido, C. Grebogi, and M. S. Baptista *Phys. Rev. E*, vol. 92, p. 062808, 2015.
- [23] H. Sakaguchi and Y. Kuramoto *Prog. Theor. Phys.*, vol. 76, p. 576, 1986.
- [24] D. M. Abrams and S. H. Strogatz *Phys. Rev. Lett.*, vol. 93, p. 174102, 2004.
- [25] A. Pikovsky and M. Rosenblum *Phys. Rev. Lett.*, vol. 101, p. 264103, 2008.
- [26] A. E. Motter *Nat. Phys.*, vol. 6, p. 164, 2010.
- [27] P. J. Davis, *Circulant Matrices*. New York: John Wiley & Sons Inc, 1979.
- [28] R. Gopal, V. K. Chandrasekar, A. Venkatesan, and M. Lakshmanan *Phys. Rev. E*, vol. 89, p. 052914, 2014.
- [29] A. Zakharova, M. Kapeller, and E. Schoöll *Phys. Rev. Lett.*, vol. 112, p. 154101, 2014.
- [30] S. Rakshit, B. K. Bera, M. Perc, and D. Ghosh *Sci. Rep.*, vol. 7, p. 2412, 2017.
- [31] M. Wolfrum and O. E. Omel'chenko *Phys. Rev. E*, vol. 84, p. 015201(R), 2011.

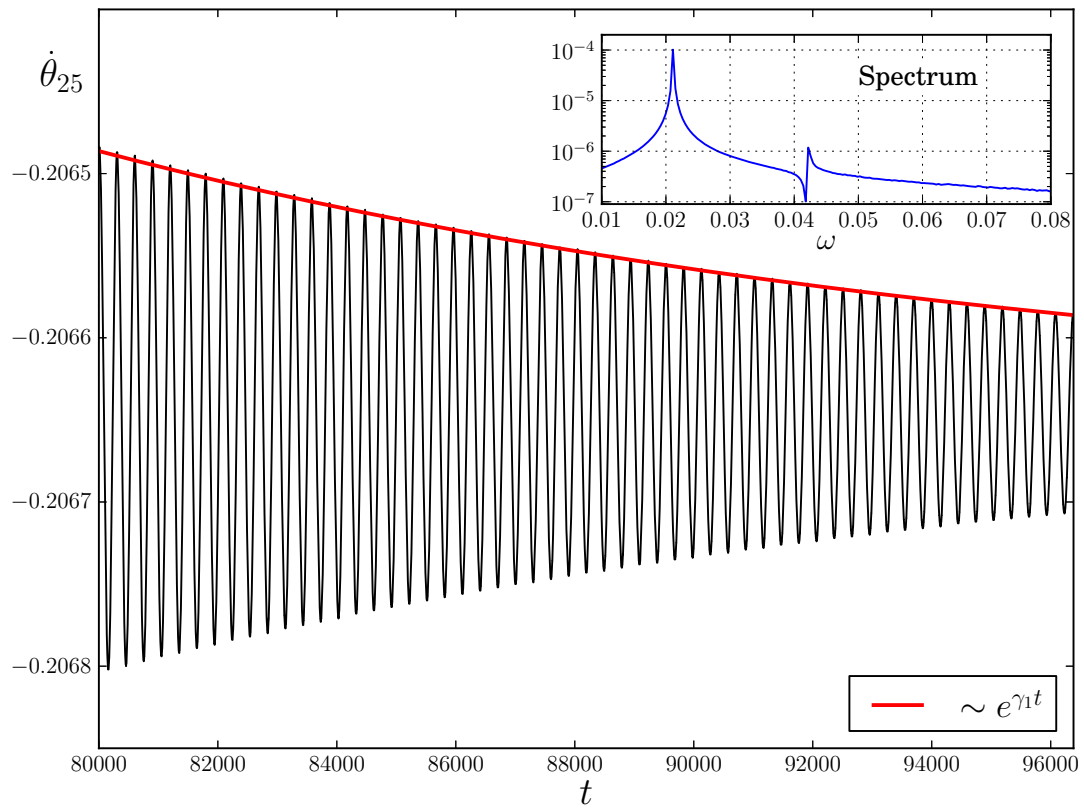


Figure 1: Behavior of $\dot{\theta}_{25}$ in the KS model for local coupling (black). The exponential decreasing curve (red) and the spectrum (blue) demonstrate the behavior of the longest-lived eigenmodes of the 8-twisted state. $N = 50$, $R = 1$, $\alpha = 1.5$, and $G_n = 0.1$.

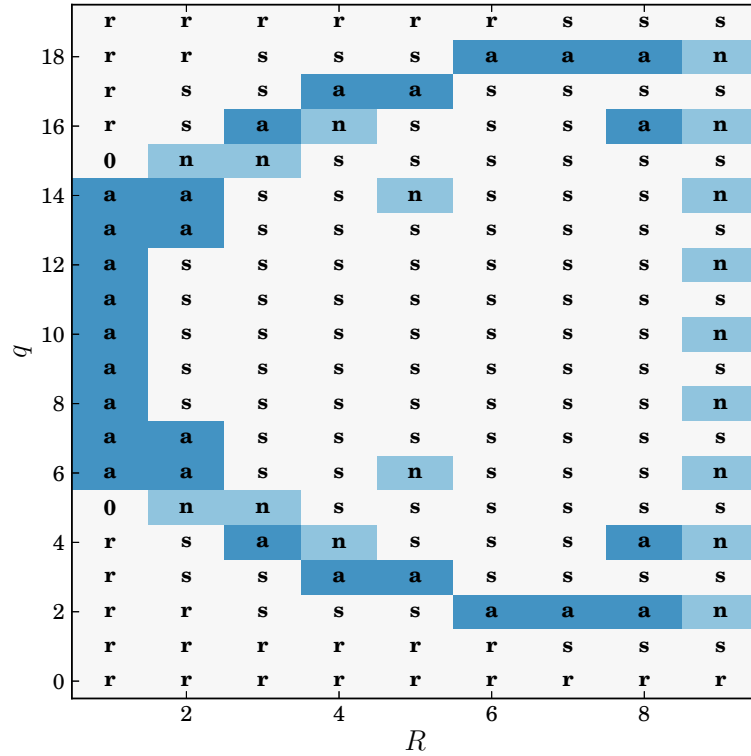
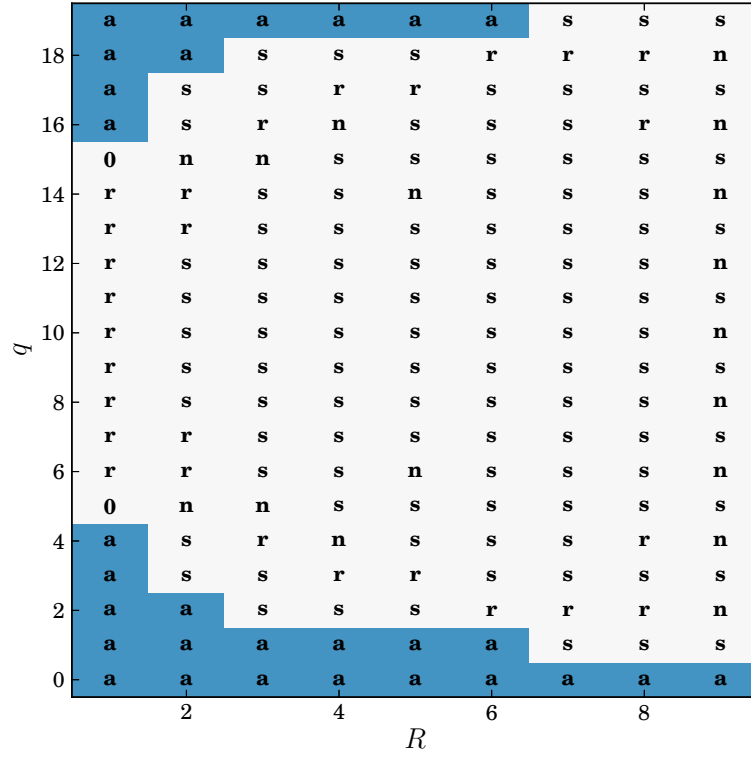


Figure 2: Stability diagrams of the q -twisted states for $N = 20$ oscillators equally coupled in a ring. Highlight for stable states: hyperbolic attractors in blue, non-hyperbolic (or neutrally) stable states in light blue; saddles, repellers and also non-hyperbolic unstable states are in white. Top: “attractive” case ($\alpha = 0$) and bottom: “repulsive” case ($\alpha = \pi$).

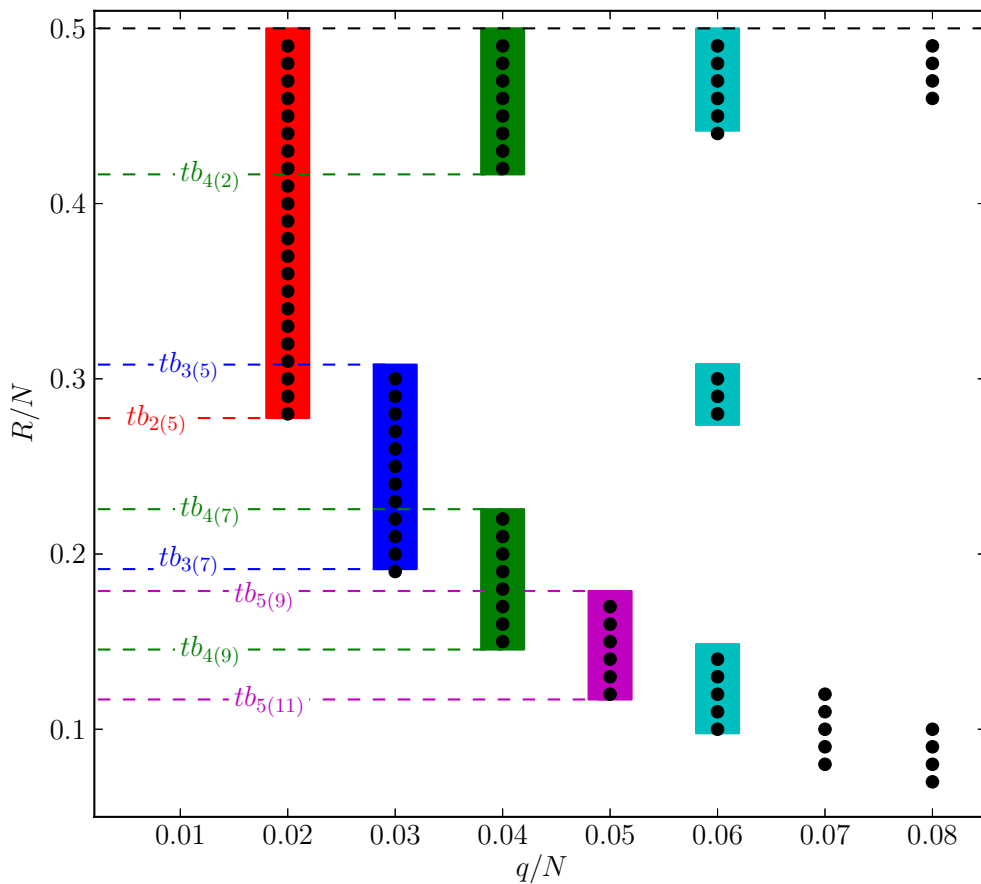


Figure 3: Stability in the repulsive regime. Black dots are the stable states for $N = 100$. Colored stripes are regions (in the continuum limit) where q -twisted states are expected to be stable, according to table 1 (For comparison, the values of q/N were calculated with $N = 100$ in both cases.).

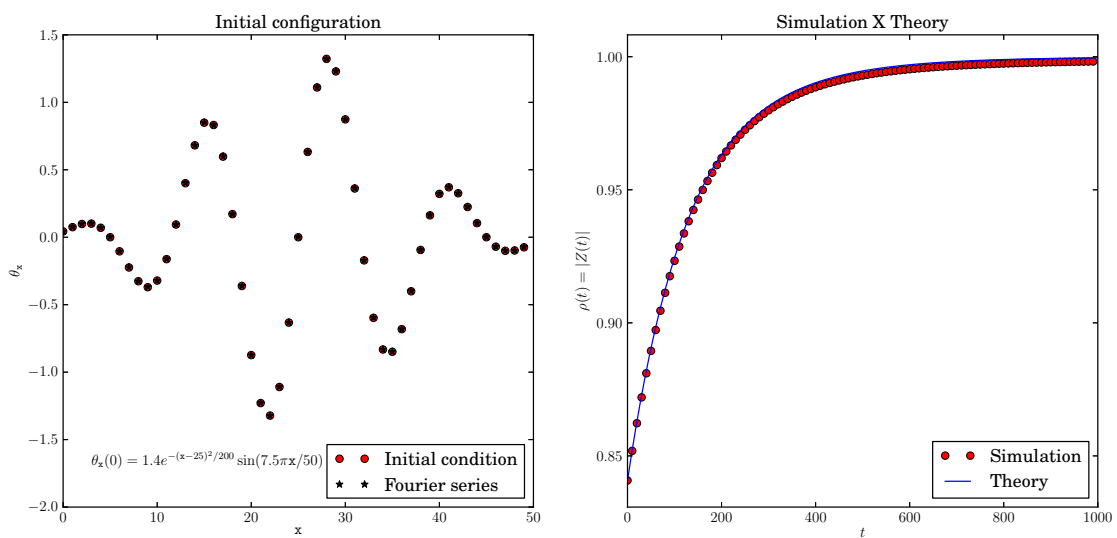


Figure 4: Left: initial configuration. Right: comparison between the theoretical prediction (obtained with Fourier decomposition and our equations for perturbations) and the results obtained by “Simulation” = numerical integration of 50 differential equations.

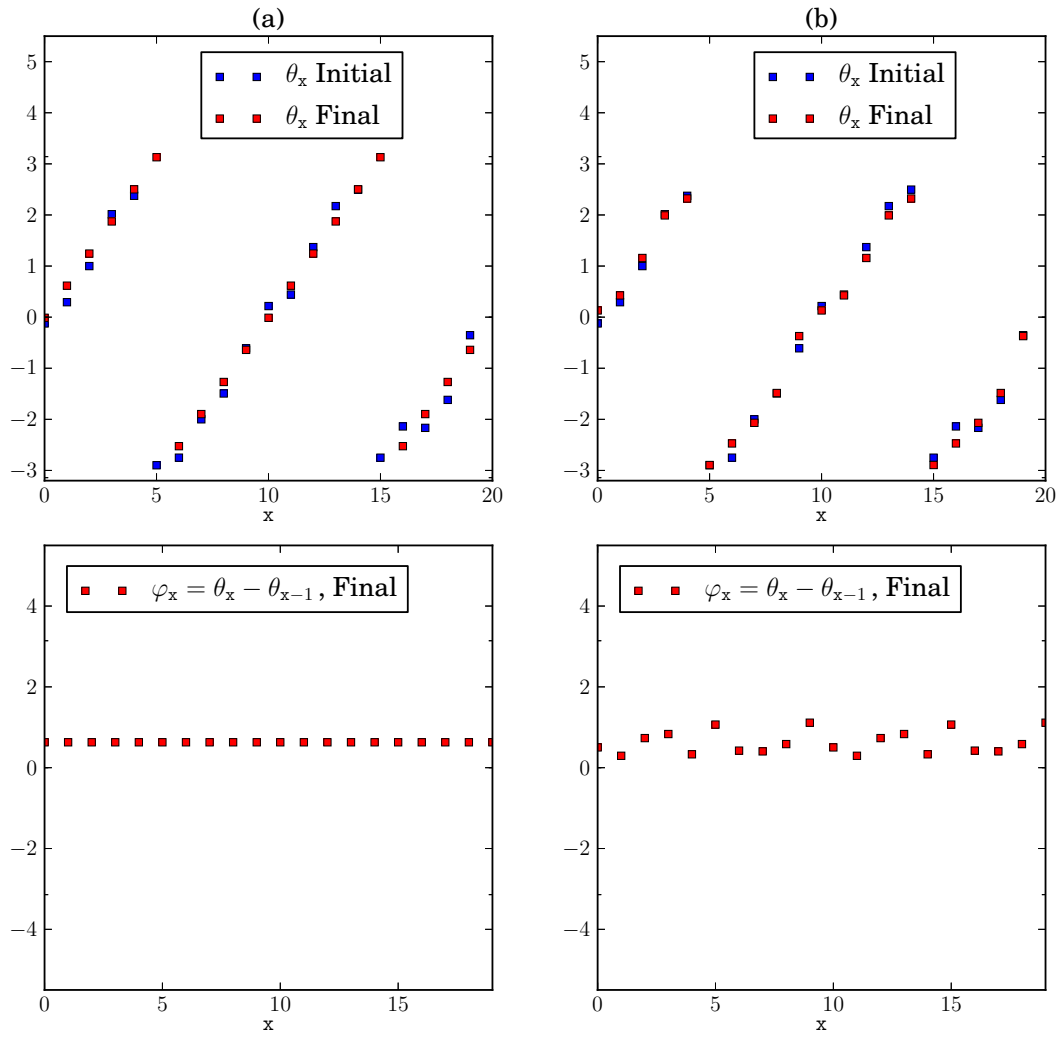


Figure 5: Signatures of the stable states in numerical simulations: (a) ($R = 8, q = 2$) is a hyperbolic attractor: homogeneous distribution of phases; (b) ($R = 9, q = 2$) is a non-hyperbolic (or neutrally) stable state: non-homogeneous distribution of phases.